Uncorrected Proof

Iran J Radiol. 2021 July; 18(3):e111704. doi: 10.5812/iranjradiol.111704.

Published online 2021 September 6. **Research Article**

Use of Cone-Beam Computed Tomography (CBCT) for Targeting the Portal Vein in Transjugular Intrahepatic Portosystemic Shunt (TIPS) Procedures: Comparison of Low-Dose with Standard-Dose CBCT

Arne Estler [1,*], Judith Herrmann [1], Christoph Artzner [1], Ruediger Hoffmann [1], Konstantin Nikolaou [2], Tobias Hepp [2], Ulrich Grosse [3], Ulrike Schempf [4], Ferdinand Seith [1] and Gerd Groezinger [1]

[1]Diagnostische und Interventionelle Radiologie, Universitätsklinikum Tübingen, Tübingen, Germany
[2]Diagnostische und Interventionelle Radiologie, Tübingen, Germany
[3]Radiologie Kantonsspital Frauenfeld, Frauenfeld, Switzerland
[4]Tübingen, Germany

[*]*Corresponding author*: Diagnostische und Interventionelle Radiologie, Universitätsklinikum Tübingen, Hoppy-SeylerSt 3, Tübingen, Germany. Email: arne.estler@med.uni-tuebingen.de

Received 2020 December 01; **Revised** 2021 June 15; **Accepted** 2021 June 19.

Abstract

Background: A transjugular intrahepatic portosystemic shunt (TIPS) is a common treatment for patients with portal hypertension. In these patients, the portal vein can be punctured under the guidance of cone-beam computed tomography (CBCT).
Objectives: To compare standard-dose (SD) CBCT with low-dose (LD) CBCT, as three-dimensional (3D) intraprocedural guidance for transhepatic puncture in TIPS placement, in terms of image quality, radiation dose, technical success, and complications.
Materials and Methods: A total of 44 patients were retrospectively enrolled in this study. Eighteen patients underwent LD-CBCT, while 26 patients underwent SD-CBCT for guiding the portal vein puncture. A quantitative assessment of image quality was performed by calculating the contrast-to-noise ratio (CNR) of the hepatic portal vein. This analysis was based on a five-point vascular visualization scale (VVS), ranging from optimal (score = 1) to non-diagnostic (score = 5), while a three-point Likert scale was used for motion artifacts (1 = no motion artifacts, 3 = blurred). Image streak artifacts were also rated from one to three, based on the image quality results. Technical success was also investigated, including the number of puncture attempts, time to successful portal vein access, and radiation dose of the TIPS procedure.
Results: Based on the results, TIPS could be placed successfully in all cases. Neither VVS (LD-CBCT VVS: 2.78, SD-CBCT VVS: 2.54; P = 0.467), nor the procedure time showed any significant differences between the groups (LD-CBCT: 48.3 min, SD-CBCT: 40.2 min; P = 0.45). Moreover, the objective evaluation of image quality indicated the lower quality of LD-CBCT images; however, the difference was not statistically significant (LD-CBCT CNR: 1.1 $\pm$ 0.76, SD-CBCT CNR: 1.3 $\pm$ 1.1; P = 0.5). The median number of puncture attempts was the same for SD-CBCT and LD-CBCT (n = 3; range: 1 - 6). Also, the mean dose area product (DAP) was significantly lower in LD-CBCT as compared to SD-CBCT (LD-CBCT: 2733 $\pm$ 848 μGm^2, SD-CBCT: 6119 $\pm$ 1677 μGm^2; P < 0.0001). The total DAP was significantly lower using LD-CBCT (LD-CBCT: 14831 $\pm$ 9299 μGm^2, SD-CBCT: 20985 $\pm$ 10127 μGm^2; P = 0.047).
Conclusion: Both SD-CBCT and LD-CBCT provided successful 3D guidance for portal vein puncture during TIPS creation. Although these methods did not differ significantly in terms of image quality, complications, or number of puncture attempts, LD-CBCT significantly reduced the radiation dose.

Keywords: Radiation, Dose Reduction, TIPS

1. Background

In patients with symptomatic portal hypertension, placement of a transjugular intrahepatic portosystemic shunt (TIPS) is a common procedure in interventional radiology (1). The main indications for TIPS include variceal bleeding and refractory ascites in portal hypertension (2, 3), which are commonly caused by underlying liver cirrhosis. The TIPS placement reliably reduces the portosystemic pressure gradient in most cases (4). Therefore, it is very effective in the treatment of ascites and varicose vein bleeding in acute cases and can be also helpful in the prevention of secondary varicose vein bleeding (2, 3). Since the portal vein cannot be visualized by fluoroscopy alone, the most critical step in TIPS placement is the transhepatic puncture of the portal vein.

Copyright © 2021, Author(s). This is an open-access article distributed under the terms of the Creative Commons Attribution-NonCommercial 4.0 International License (http://creativecommons.org/licenses/by-nc/4.0/) which permits copy and redistribute the material just in noncommercial usages, provided the original work is properly cited.

Uncorrected Proof

For periprocedural planning in transhepatic puncture, there are several methods to visualize the portal vein. Wedged portograms with iodinated contrast medium or carbon dioxide, besides transsplenic or transarterial mesenteric indirect portography, can be used to visualize the portal vein indirectly (5, 6). The portal vein can be also directly visualized and targeted by transabdominal or intravascular ultrasound (IVUS) (7, 8). However, the use of transabdominal ultrasound has several limitations, such as the need for creating favorable sonographic conditions and non-standard imaging planes. Besides, an assistant is needed to handle the ultrasound probe during the procedure.

Real-time three-dimensional (3D) mapping of the portal vein branches, using contrast-enhanced (CE) C-arm computed tomography (CT), has been introduced as a promising tool for guiding punctures. Not only is portal vein mapping technically feasible, but also it causes a significant reduction in the intervention time with a low complication rate (1, 7, 9, 10). Cone-beam computed tomography (CBCT) uses a C-arm with a flat-panel detector, along with the corresponding software, to create markers on cross-sectional images, which can be used as an overlay for real-time 3D guidance in the portal vein. Besides, fusion of pre-interventional magnetic resonance imaging (MRI) or CT with intraprocedural CBCT is possible (11).

On the other hand, one of the limitations of the widespread use of CBCT is the significant radiation dose (10, 12). For image acquisition, different CBCT protocols are available. Differences between these protocols are mainly related to radiation dose and acquisition time, although there are some differences in the C-arm positioning, number of frames per rotation, and field of view (FOV). In this regard, Ketelsen et al. acquired 397 CBCT images (6 sec/slice) at a detector input dose of 0.36 μGy/image and an angular increment of 0.5°/image, with a 200° orbit around the patient (1). In comparison, Boning et al. (10) acquired 312 projections within 10 seconds during a 180° - 240° rotation.

Unlike the mentioned high-dose protocols, there are CBCT protocols that use fewer frames ($n \leq 200$), resulting in a shorter acquisition time and consequently, fewer respiratory motion artifacts; this increases the image quality and patient comfort. On the other hand, the lower radiation dose may result in a lower contrast-to-noise ratio (CNR), which can produce non-diagnostic images. The principle of radiation protection "as low as reasonably achievable" (ALARA) (13) is generally valid.

2. Objectives

This study aimed to compare standard-dose CBCT with low-dose CBCT for TIPS guidance in terms of technical success, complications, radiation dose, and image quality.

3. Materials and Methods

3.1. Patient Selection

This retrospective study was approved by the institutional ethics board. The inclusion criteria were as follows: (1) Symptomatic portal hypertension and refractory ascites or recurrent variceal bleeding; (2) age of 18 years or above; and (3) interdisciplinary approval of TIPS placement. On the other hand, the exclusion criteria were contraindications to TIPS, such as pregnancy or hepatic encephalopathy.

Patients were recruited from December 2014 to September 2019, where the physician could choose between LD-CBCT and SD-CBCT, according to the patient's stature and anatomical features (LD-CBCT available since 2018). Finally, 44 consecutive patients underwent SD-CBCT or LD-CBCT as part of the TIPS insertion procedure (mean age: 60.0 $\pm$ 17, age range: 18 - 81; 70% male). Informed consent was obtained from each patient for the TIPS procedure.

3.2. TIPS Procedure

The TIPS procedure was performed as described by Ketelsen et al. (1). All TIPS procedures were performed by a senior interventional radiologist with at least six years of experience in interventional radiology. All procedures were performed under general anesthesia, and paracentesis was performed before the procedure. A 10 French sheath was inserted into the right jugular vein and placed in the right hepatic vein. Next, contrast-enhanced CBCT was performed in an arms-down positioning, and the portal vein branches were mapped. After 3D guided puncture of the portal vein, aspiration of blood with the TIPS needle and subsequent contrast injection confirmed successful portal vein puncture. Following the successful portal vein puncture, a standard TIPS stent graft (Viatorr, W.L. Gore, Arizona, USA) was used to secure the TIPS tract. Technical success was defined as successful contrast injection into the portal vein via cannulation with a 4F diagnostic catheter. Later, the portosystemic gradient was lowered to 10 mmHg or less (3, 14).

3.3. Image Acquisition and Planning of Transhepatic Puncture During the TIPS Procedure

All CBCT procedures were performed using a single, robotic, single-axis, angiographic C-arm system (Artis Zeego with Q-Technology, Siemens Healthcare GmbH, Forchheim, Germany). The CBCT images were acquired based on a standardized contrast injection protocol in

Uncorrected Proof

all C-arm CT scans via peripheral vein access (18G). The injection protocol included venous administration of diluted contrast medium (75 mL of Ultravist at 370 mg/mL; Bayer Schering, Zürich, Switzerland), followed by a saline flush injected by an automated power injector (Accutron-HP-D, Medtron, Saarbrücken, Germany) at a flow rate of 4.5 mL/second. The C-arm CT system was set to start automatically after 60 seconds.

The rotation time for CBCT was either three seconds (LD-CBCT) or six seconds (SD-CBCT). The images were acquired at a rate of 60 frames/second in both acquisition methods. Details of different CBCT protocols are presented in Table 1. The CBCT system acquired 397 projection images in SD-CBCT and 167 projection images in LD-CBCT at a detector entrance dose of 0.36 μGy/frame (angular increment of 0.5°/frame for SD-CBCT and 1.2°/frame for LD-CBCT) on a 200° circular trajectory. The CBCT images were acquired using the breath-holding technique. The kV plateau was 90 kVp, and the FOV was 48 cm, with a voxel matrix of 512 × 512. In SD-CBCT, a 3D eccentric 7 × 7 kernel was used, while a non-eccentric 7 × 7 kernel was applied in LD-CBCT. The images were then reconstructed as multiplanar reconstruction (MPR) images.

Table 1. Imaging Parameters of CBCT Acquisitions

Imaging parameters	LD-CBCT group (n = 18)	SD-CBCT group (n = 26)
Rotation time, sec	3	6
Acquisition rate, frames/sec	60 frames/sec	60
Images acquired	167	397
Detector entrance dose, μGy/frame	0.36	0.36
Angular increment, °/frame	1.2	0.5
Power source, kVp	90	90
Field of view, cm	48	48
Voxel matrix	512 × 512	512 × 512
Kernel	Non-eccentric kernel (7 × 7)	Eccentric 3D kernel (7 × 7)

Abbreviations: LD-CBCT, low-dose cone-beam computed tomography; SD-CBCT, standard-dose cone-beam computed tomography.

During the intervention, 3D fluoroscopy guidance was used to plan the virtual needle trajectory by specifying four markers in the main portal vein (Figure 1) (1). After planning, the virtual needle trajectory was superimposed with 2D fluoroscopy. If necessary, the needle trajectory was visualized from different angles (anterior-posterior and oblique views) to target the superimposed 3D markers in the fluoroscopy image. For a retrospective analysis of CBCT images, MPR reconstruction was performed.

3.4. Clinical Outcome Assessment

In both groups, several parameters were determined: the number of attempts for the portal vein puncture, periprocedural complications, pre- and post-interventional portosystemic pressure gradients, and radiation dose (dose-area product [DAP] according to angiography) in the entire procedure and CBCT, respectively. Moreover, the procedure time, time until successful transhepatic puncture of the portal vein (procedure time until the first image acquisition of the portal diagram), and body mass index (BMI) were assessed.

3.5. Assessment of Image Quality

3.5.1. Quantitative Evaluation of Image Quality

To quantify the quality of CBCT images, the CNR was measured. Three different regions of interest (ROIs) were placed in the right portal vein at different axial slices and in the surrounding liver parenchyma (n = 3) as background (Figure 2). The CNR was calculated as previously described (15):

$$CNR = \frac{(Mean\ HU\ Liver - Mean\ HU\ Portal\ vein)}{Mean\ SD\ HU\ Liver} \quad (1)$$

3.5.2. Qualitative Evaluation of Image Quality

Two board-certified interventional radiologists, with at least six years of experience in interventional radiology using CBCT, evaluated the images in a random order and reached a consensus. None of the radiologists were involved in the initial treatment of patients, and they were blinded to the type of image acquisition (LD-CBCT vs. SD-CBCT) and clinical cases. To reduce bias in the evaluation of image quality, the images were shown to the radiologists in a random order. The qualitative evaluation of image quality was conducted, based on a five-point vessel visualization scale (VVS), ranging from optimal visualization (score = 1) to non-diagnostic visualization (score = 5). Streak artifacts were also rated from one (none) to three (significant), based on the image quality. Besides, a three-point Likert scale was used for evaluating the motion artifacts (1 = no motion artifacts, 3 = blurred).

3.6. Statistical Analysis

IBM SPSS version 25 (IBM, Armonk, NY, USA) was used for statistical analysis. A two-tailed P-value less than 0.05 was considered statistically significant. After verification of non-Gaussian distribution by Shapiro-Wilk test, we performed a non-parametric test (Mann-Whitney U-test) to assess the significance level. Post-hoc Dunn-Bonferroni tests

Uncorrected Proof

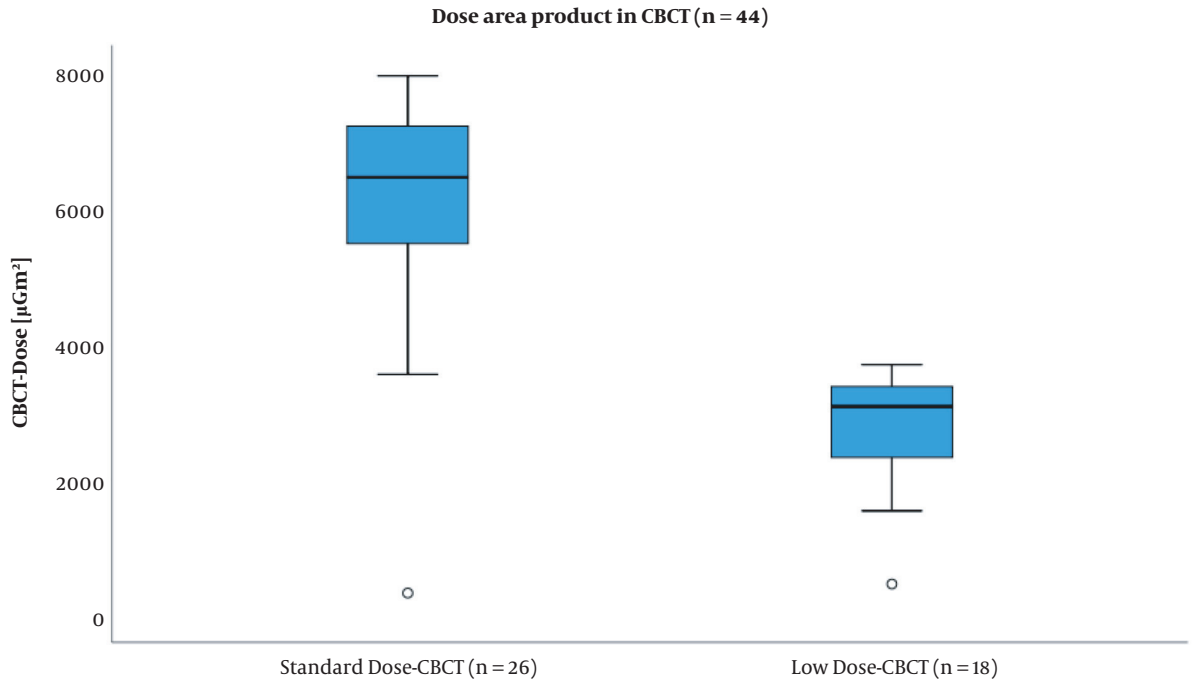


Figure 1. The dose area product (DAP) of SD-CBCT versus LD-CBCT. Data is presented as median ± SD. The mean DAP of LD-CBCT was significantly lower than that of SD-CBCT (LD-CBCT: 2733 ± 848 μGm^2, SD-CBCT: 6119 ± 1677 μGm^2; P < 0.0001).

were also performed to differentiate the groups. The results are presented as mean ± standard deviation (SD).

4. Results

4.1. Patients

A total of 44 patients were enrolled in this study. Overall, 18 patients were assigned to the LD-CBCT group and 26 patients to the SD-CBCT group. The mean age of the patients was 60.0 ± 17.0 years (range: 18 - 81 years), and 70.0% of them were male. The BMI did not differ significantly between the two groups (LD-CBCT: 24.3 ± 5.5 kg/m² vs. SD-CBCT: 25.6 ± 4.2 kg/m²; P = 0.4). The patient data is presented in Table 2.

4.2. Periprocedural Outcomes

No major periprocedural or postprocedural complications were observed in any of the patients undergoing the TIPS procedure (n = 44). Three-dimensional CBCT mapping of the portal vein for the subsequent puncture of the portal vein and TIPS placement was feasible in all cases. The average number of puncture attempts was 2.5 ± 1.7 (median: 3; range: 1 - 6) in the LD-CBCT group and 3.0 ± 1.6 (median: 3, range: 1 - 6) in the SD-CBCT group (P = 0.8), with one to six punctures in each group. In all patients, the portosystemic pressure gradient was reduced to 10 mmHg or less.

Before the TIPS implantation, the portosystemic pressure gradient was 17.8 ± 5.2 mmHg in the LD-CBCT group, while it reduced to 5.11 ± 2.0 mmHg after a technically successful procedure (SD-CBCT: 19.7 ± 5.0 mmHg and 5.0 ± 2.4 mmHg, respectively). There was no significant difference in the time interval from the onset of the procedure until successful puncture of the portal vein (procedure time from the beginning of the intervention until visualization of the portal vein). The mean time gap was 48.3 ± 42.1 minutes in the LD-CBCT group and 40.2 ± 18.2 minutes in the SD-CBCT group (P = 0.45).

Based on the findings, the mean DAP was significantly lower in the LD-CBCT group compared to the SD-CBCT group (LD-CBCT: 2733 ± 848 μGm^2, SD-CBCT: 6119 ± 1677 μGm^2; P < 0.0001). Also, the total dose of the procedure was significantly lower when using LD-CBCT (LD-CBCT: 14831 ± 9299 μGm^2, SD-CBCT: 20985 ± 10127 μGm^2; P = 0.047). The results are presented in Table 3 and Figures 3 and 4.

4.3. Quantitative Analysis of Image Quality

The TIPS procedure was successfully planned and performed for all patients, based on the acquired CBCT im-

Uncorrected Proof

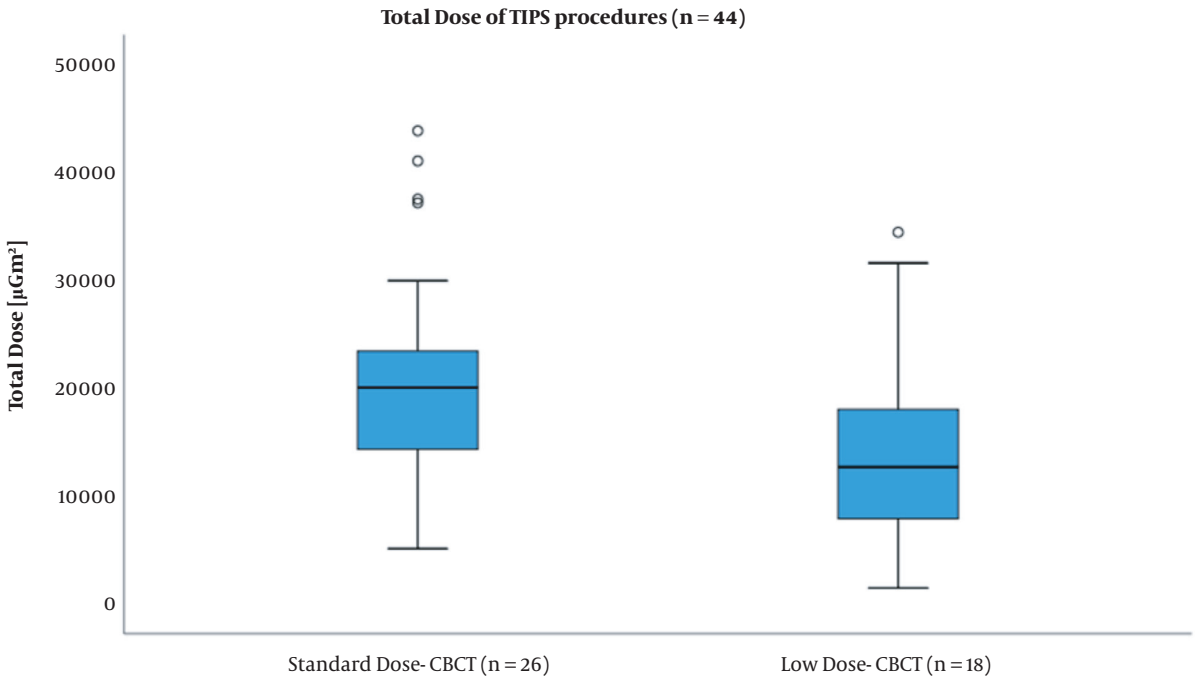


Figure 2. The box plot of total radiation dose area product (DAP) during a transjugular intrahepatic portosystemic shunt (TIPS) procedure under the guidance of SD-CBCT and LD-CBCT. The total dose in the procedure was also significantly lower using LD-CBCT (LD-CBCT: 14831 ± 9299 μGm^2, SD-CBCT: 20985 ± 10127 μGm^2; P = 0.047).

ages. The objective evaluation of the CBCT image quality by CNR measurements showed a slightly lower image quality in LD-CBCT compared to SD-CBCT; however, the difference was not statistically significant (mean CNRLD-CBCT: 1.1 ± 0.76, mean CNRSD-CBCT: 1.3 ± 1.1; P = 0.5). The mean VVS also did not show any significant differences between the groups (VVSLD-CBCT: 2.78 ± 1.2; VVSSD-CBCT: 2.54 ± 1.0; P = 0.467). Moreover, based on the image quality, motion artifacts were rated from one to three (1 = none to 3 = significant): mean MALD-CBCT: 1.29 ± 0.47 and mean MASD-CBCT: 1.79 ± 0.43 (P = 0.837). The results of quantitative image analysis are presented in Table 4.

5. Discussion

Liver cirrhosis is a serious cause of mortality with a 10-year mortality rate of 30% - 60% (16). Since the majority of liver cirrhosis cases are associated with portal hypertension, many patients can benefit from the TIPS procedure (3). Generally, TIPS is an established procedure for the treatment of complications of portal hypertension, as it reliably reduces the portosystemic pressure gradient (4). The most challenging step in TIPS placement is transhepatic portal vein puncture, which can be performed using various imaging techniques.

Multiple techniques have been employed for transhepatic portal vein catheterization, including superior mesenteric artery angiography, transabdominal ultrasound guidance, and wedged portography with carbon dioxide or iodized contrast medium (17-21). Despite improvements in imaging techniques, most procedural complications of TIPS are related to failed puncture attempts of the portal vein (3). The 3D real-time mapping of the portal vein branches by intravenous contrast-enhanced CBCT, introduced by Ketelsen et al. (1), is a relatively new technique. The targeted puncture of the portal vein under accurate needle guidance is facilitated by the projection of 3D markers onto the real-time fluoroscopic image. Consequently, complex vascular and anatomical structures can be visualized, and periprocedural planning of the needle path can be facilitated (22-24).

However, the DAP of CBCT suggests a significant radiation dose (9, 10), which is higher than that of conventional TIPS, as shown by Ketelsen et al. (1). This finding is of particular importance, because patients receiving TIPS may have an improved prognosis, compared to patients with liver cirrhosis not receiving TIPS (25). Especially in young pa-

Uncorrected Proof

Table 2. The Patients' Characteristics in the Two Groups

Patients' characteristics	LD-CBCT group (n = 18)	SD-CBCT group (n = 26)	P-value
Mean age (± SD), y	58 ± 13	56 ± 16	0.54
Sex (No. of patients)			0.66
Male	12	19	
Female	6	7	
Mean BMI (± SD)	24.3 ± 5.5	25.6 ± 4.2	0.43
Indications for TIPS (No. of patients)			
Therapy-refractory ascites	12	17	0.93
Hepatorenal syndrome	1	0	0.51
Variceal bleeding	4	6	0.54
Budd-Chiari syndrome	1	3	0.20
Child-Pugh score			
A	8	7	0.52
B	6	14	0.19
C	3	2	0.37
Unknown	1	3	0.20
Cause of cirrhosis			
Alcoholism	11	15	0.83
Autoimmune disorder	1	2	0.79
Cryptogenic	5	2	0.11
Primary sclerosing cholangitis	0	2	0.16
Non-alcoholic steatosis hepatis	0	2	0.16
Budd-Chiari syndrome	1	3	0.20
Encephalopathy	0	0	NA

Abbreviations: LD-CBCT, low-dose cone-beam computed tomography; SD-CBCT, standard-dose cone-beam computed tomography.

Table 3. Detailed Information of Median Puncture Attempts, Mean Portosystemic Pressure Gradient Before and After TIPS, Mean Procedural Time, and DAP of CBCT and the Whole Procedure[a, b]

Characteristics	LD-CBCT group (n = 18)	SD-CBCT group (n = 26)	P-value
Mean number of puncture attempts	2.5 ± 1.7	3.0 ± 1.6	0.8
Mean portosystemic pressure gradient before TIPS	17.8 ± 5.2	19.7 ± 5.0	0.23
Mean portosystemic pressure gradient after TIPS	5.11 ± 2.0	5.0 ± 2.4	0.87
Mean procedural time, min	48.3 ± 42.1	40.2 ± 18.2	0.45
Mean DAP for CBCT, μGm^2	2733 ± 848	6119 ± 1677	< 0.0001
Total DAP, μGm^2	14831 ± 9299	20985 ± 10127	0.047

Abbreviations: LD-CBCT, low-dose cone-beam computed tomography; SD-CBCT, standard-dose cone-beam computed tomography.
[a] Values are expressed as mean ± SD.
[b] The median puncture attempts and the mean procedural time were not significantly different between the groups. The mean DAP of CBCT and the total intervention dose were significantly different between the groups.

tients with a long life expectancy, this radiation dose may be a cause of concern, despite an early need for TIPS (e.g., patients with Budd-Chiari syndrome (26)).

With regard to patient radiation, the use of LD-CBCT can be a promising approach. In this study, the use of LD-CBCT (3-sec image acquisition time) for TIPS guidance was

Uncorrected Proof

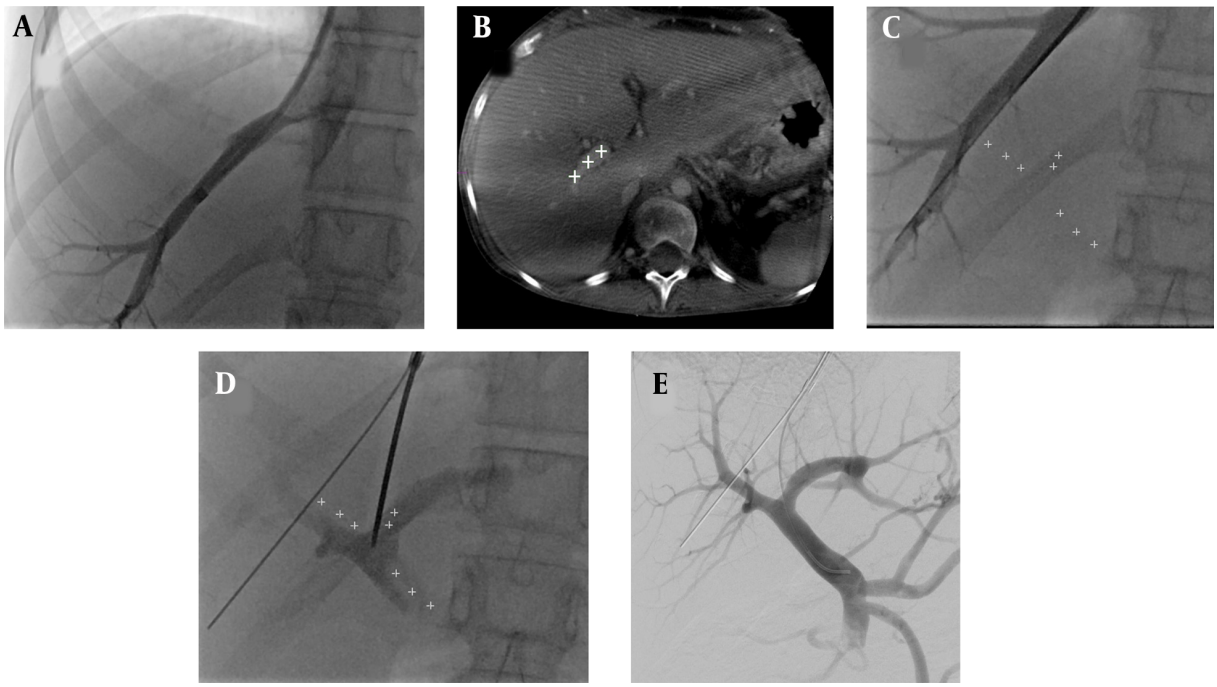


Figure 3. A, Hepatic venogram; B, Based on 3D-CBCT, the portal vein was marked; C, After 3D mapping of the right portal vein branch in C-arm CT, the annotated portal vein branches were overlaid on the real-time fluoroscopic image; D, After puncture of the portal vein, the contrast medium was injected to confirm successful puncture; E, Portography shows the patent portal vein with hepatopetal flow and retrograde filling of the splenic and inferior mesenteric veins.

Table 4. The Results of Quantitative Image Analysis[a]

Characteristics	LD-CBCT group (n = 18)	SD-CBCT group (n = 26)	P-value
Mean CNR	1.1 ± 0.76	1.3 ± 1.1	0.5
Mean VVS	2.78 ± 1.2	2.54 ± 1.0	0.467

Abbreviations: CBCT, cone-beam computed tomography; CNR, contrast-to-noise ratio; VVS, vessel visualization score.
[a]Values are expressed as mean ± SD.

investigated and compared with SD-CBCT (6-sec image acquisition time). It was found that LD-CBCT reduced the radiation dose by almost 50% compared to SD-CBCT, without compromising the clinical application or significant differences in image quality; on the other hand, the radiation dose of SD-CBCT was comparable to the report by Ketelsen et al. (1). Besides, no significant difference was found between the two groups regarding the time required for successful puncture of the portal vein and the median number of portal vein puncture attempts.

In the present study, the effect of BMI on the radiation dose was non-significant, as both groups showed approximately the same mean BMI with robust image quality (mean BMI of LD-CBCT group: 24.3 ± 5.5 kg/m^2; mean BMI of SD-CBCT group: 25.6 ± 4.2 kg/m^2). Due to the longer recording time, motion artifacts are expected to be more pronounced in 6-sec SD-CBCT images. However, motion artifacts did not play a significant role in our clinical setting, as apnea can occur in patients under general anesthesia over a long period. Therefore, no significant difference was found in motion artifacts between the groups; nevertheless, in patients without general anesthesia, holding breath even for six seconds can be challenging.

In 2015, Ketelsen et al. (1) demonstrated that 3D-CBCT guidance for the TIPS procedure significantly reduced the procedural time and radiation dose, as well as the number of puncture attempts, as compared to TIPS creation using wedged portography as guidance. In this study, different methods of portal vein visualization (wedged portography vs. CBCT) were compared, and a mean DAP of 6160 ± 1380 μGm^2 was recorded in CBCT (median puncture attempts: 2 ± 1.3); these results are consistent with our findings based on SD-CBCT.

More recently, Böning et al. (10) reported a median of

Uncorrected Proof



Figure 4. Measurement of the contrast-to-noise ratio (CNR) within the right portal vein against the background liver parenchyma. Three measurements were performed in the portal vein and the liver in different axial slides. C-arm CT images present an optimal visualization of the main portal vein, as well as the proximal right portal vein. The portal vein branches were subsequently marked with an annotation tool and overlaid on a real-time fluoroscopic image.

two puncture attempts in CBCT, which is in the same range as ours. Also, the mean puncture time in previous studies is comparable to the present work (Boning et al.: 32 $\pm$ 45 min; Ketelsen et al.: 32.6 $\pm$ 22.7 min; the present study: SD-CBCT, 40 $\pm$ 18 min and LD-CBCT, 48 $\pm$ 42 min). However, the use of LD-CBCT could especially lower the radiation dose in our study, compared to previous reports (Boning et al. (10): 56300 $\pm$ 28900 μGm^2; Ketelsen et al. (1): 188169 $\pm$ 121180 μGm^2; the present study: LD-CBCT, 14831 $\pm$ 9299 μGm^2 and SD-CBCT, 20985 $\pm$ 10127 μGm^2).

The limitations of this study include the small population and the retrospective design of the study, which might limit the generalizability of our results. Also, CBCT during TIPS is a particular type of procedure, as many interventionalists use ultrasound or indirect portography for visualization of the portal vein. However, since these procedures could not be performed for any of our patients due to poor image quality, LD-CBCT was introduced as a promising approach for all patients meeting the requirements. Generally, the patient's size plays a major role in LD-CBCT, since the rotation method of C-arm, with the C-arm axis rotating along the longitudinal axis of the patient, limits image acquisition in obese patients (BMI > 30 kg/m^2). Besides, in this study, for extremely obese patients, SD-CBCT was used because of the previously known high image quality to avoid a potential repetition of image acquisition in possibly non-diagnostic images. Besides, since a standard amount of diluted contrast medium was used, future studies can use adjusted contrast medium doses in different BMI groups and CBCT dose protocols.

In conclusion, LD-CBCT is a suitable alternative to SD-CBCT during CBCT-guided TIPS procedures, and the patient radiation dose can be significantly reduced. Besides, due to the shorter acquisition time in LD-CBCT, it is possible to

Uncorrected Proof

diminish motion artifacts, as breath holding must be done for a shorter time.

Footnotes

Authors' Contributions: Study concept and design: Gerd Grözinger and Arne Estler. Acquisition of data: Arne Estler, Christoph Artzner, Ulrike Schempf, Ulrich Grosse, Ferdinand Seith, Judith Herrmann, and Ruediger Hoffmann. Analysis and interpretation of data: Arne Estler. Drafting of the manuscript: Arne Estler. Critical revision of the manuscript for important intellectual content: Gerd Grözinger, Arne Estler, Christoph Artzner, and Konstantin Nikolaou. Statistical analysis: Arne Estler and Tobias Hepp. Administrative, technical, and material support: Tobias Hepp and Gerd Grözinger. Study supervision: Gerd Grözinger.

Conflict of Interests: None.

Ethical Approval: The ethical approval code was 605/2019BO2 (https://www.medizin.uni-tuebingen.de/de/medizinische-fakultaet/ethikkommission).

Funding/Support: None.

Informed Consent: Informed consent was obtained from each patient for the TIPS procedure.

References

1. Ketelsen D, Groezinger G, Maurer M, Lauer UM, Grosse U, Horger M, et al. Three-dimensional C-arm CT-guided transjugular intrahepatic portosystemic shunt placement: Feasibility, technical success and procedural time. *Eur Radiol*. 2016;**26**(12):4277–83. doi: 10.1007/s00330-016-4340-4. [PubMed: 27048535].
2. Rossle M, Haag K, Ochs A, Sellinger M, Noldge G, Perarnau JM, et al. The transjugular intrahepatic portosystemic stent-shunt procedure for variceal bleeding. *N Engl J Med*. 1994;**330**(3):165–71. doi: 10.1056/NEJM199401203300303. [PubMed: 8264738].
3. Fidelman N, Kwan SW, LaBerge JM, Gordon RL, Ring EJ, Kerlan RJ. The transjugular intrahepatic portosystemic shunt: an update. *AJR Am J Roentgenol*. 2012;**199**(4):746–55. doi: 10.2214/AJR.12.9101. [PubMed: 22997364].
4. Grozinger G, Wiesinger B, Schmehl J, Kramer U, Mehra T, Grosse U, et al. Portosystemic pressure reduction achieved with TIPPS and impact of portosystemic collaterals for the prediction of the portosystemic-pressure gradient in cirrhotic patients. *Eur J Radiol*. 2013;**82**(12):2258–64. doi: 10.1016/j.ejrad.2013.08.017. [PubMed: 24029160].
5. Krajina A, Lojik M, Chovanec V, Raupach J, Hulek P. Wedged hepatic venography for targeting the portal vein during TIPS: comparison of carbon dioxide and iodinated contrast agents. *Cardiovasc Intervent Radiol*. 2002;**25**(3):171–5. doi: 10.1007/s00270-001-0096-5. [PubMed: 12058211].
6. Miyazono N, Inoue H, Ueno K, Nishida H, Kanetsuki I, Miyake S, et al. [Evaluation of anastomosis between intrahepatic or extrahepatic vessels by intra-arterial digital subtraction angiography using carbon dioxide]. *Nihon Igaku Hoshasen Gakkai Zasshi*. 1995;**55**(5):289–95. Japanese. [PubMed: 7784148].
7. Tavare AN, Wigham A, Hadjivassilou A, Alvi A, Papadopoulou A, Goode A, et al. Use of transabdominal ultrasound-guided transjugular portal vein puncture on radiation dose in transjugular intrahepatic portosystemic shunt formation. *Diagn Interv Radiol*. 2017;**23**(3):206–10. doi: 10.5152/dir.2016.15601. [PubMed: 28223261]. [PubMed Central: PMC5411001].
8. Farsad K, Kaufman JA. Novel Image Guidance Techniques for Portal Vein Targeting During Transjugular Intrahepatic Portosystemic Shunt Creation. *Tech Vasc Interv Radiol*. 2016;**19**(1):10–20. doi: 10.1053/j.tvir.2016.01.002. [PubMed: 26997085].
9. Tacher V, Petit A, Derbel H, Novelli L, Vitellius M, Ridouani F, et al. Three-dimensional Image Fusion Guidance for Transjugular Intrahepatic Portosystemic Shunt Placement. *Cardiovasc Intervent Radiol*. 2017;**40**(11):1732–9. doi: 10.1007/s00270-017-1699-9. [PubMed: 28516271].
10. Boning G, Ludemann WM, Chapiro J, Jonczyk M, Hamm B, Gunther RW, et al. Clinical Experience with Real-Time 3-D Guidance Based on C-Arm-Acquired Cone-Beam CT (CBCT) in Transjugular Intrahepatic Portosystemic Stent Shunt (TIPSS) Placement. *Cardiovasc Intervent Radiol*. 2018;**41**(7):1035–42. doi: 10.1007/s00270-018-1877-4. [PubMed: 29541837].
11. Luo X, Wang X, Zhao Y, Ma H, Ye L, Yang L, et al. Real-Time 3D CT Image Guidance for Transjugular Intrahepatic Portosystemic Shunt Creation Using Preoperative CT: A Prospective Feasibility Study of 20 Patients. *AJR Am J Roentgenol*. 2017;**208**(1):W11–6. doi: 10.2214/AJR.15.15210. [PubMed: 27786554].
12. Braak SJ, Strijen van M, Meijer E, Heesewijk van J, Mali W. Operator Radiation Exposure in Cone-Beam Computed Tomography Guidance. *J Belg Soc Radiol*. 2016;**100**(1):40. doi: 10.5334/jbr-btr.816. [PubMed: 30038979]. [PubMed Central: PMC5854453].
13. Strauss KJ, Kaste SC. The ALARA (as low as reasonably achievable) concept in pediatric interventional and fluoroscopic imaging: striving to keep radiation doses as low as possible during fluoroscopy of pediatric patients–a white paper executive summary. *Radiology*. 2006;**240**(3):621–2. doi: 10.1148/radiol.2403060698. [PubMed: 16926319].
14. Kothary N, Abdelmaksoud MH, Tognolini A, Fahrig R, Rosenberg J, Hovsepian DM, et al. Imaging guidance with C-arm CT: prospective evaluation of its impact on patient radiation exposure during transhepatic arterial chemoembolization. *J Vasc Interv Radiol*. 2011;**22**(11):1535–43. doi: 10.1016/j.jvir.2011.07.008. [PubMed: 21875814].
15. Bongers MN, Bier G, Kloth C, Schabel C, Fritz J, Nikolaou K, et al. Improved Delineation of Pulmonary Embolism and Venous Thrombosis Through Frequency Selective Nonlinear Blending in Computed Tomography. *Invest Radiol*. 2017;**52**(4):240–4. doi: 10.1097/RLI.0000000000000333. [PubMed: 27861205].
16. Sorensen HT, Thulstrup AM, Mellemkjar L, Jepsen P, Christensen E, Olsen JH, et al. Long-term survival and cause-specific mortality in patients with cirrhosis of the liver: a nationwide cohort study in Denmark. *J Clin Epidemiol*. 2003;**56**(1):88–93. doi: 10.1016/s0895-4356(02)00531-0. [PubMed: 12589875].
17. Longo JM, Bilbao JI, Rousseau HP, Joffre FG, Vinel JP, Garcia-Villarreal L, et al. Color Doppler-US guidance in transjugular placement of intrahepatic portosystemic shunts. *Radiology*. 1992;**184**(1):281–4. doi: 10.1148/radiology.184.1.1609093. [PubMed: 1609093].
18. Adamus R, Pfister M, Loose RW. Enhancing transjugular intrahepatic portosystemic shunt puncture by using three-dimensional path planning based on the back projection of two two-dimensional portographs. *Radiology*. 2009;**251**(2):543–7. doi: 10.1148/radiol.2512080423. [PubMed: 19401578].
19. Kew J, Davies RP. Intravascular ultrasound guidance for transjugular intrahepatic portosystemic shunt procedure in a swine model. *Cardiovasc Intervent Radiol*. 2004;**27**(1):38–41. doi: 10.1007/s00270-003-2634-9. [PubMed: 15109227].

Uncorrected Proof

20. Petersen B, Binkert C. Intravascular ultrasound-guided direct intrahepatic portacaval shunt: midterm follow-up. *J Vasc Interv Radiol*. 2004;**15**(9):927–38. doi: 10.1097/01.RVI.0000133703.35041.42. [PubMed: 15361560].
21. Kee ST, Rhee JS, Butts K, Daniel B, Pauly J, Kerr A, et al. 1999 Gary J. Becker Young Investigator Award. MR-guided transjugular portosystemic shunt placement in a swine model. *J Vasc Interv Radiol*. 1999;**10**(5):529–35. doi: 10.1016/s1051-0443(99)70078-3. [PubMed: 10357476].
22. Tsauo J, Luo X, Ye L, Li X. Three-dimensional path planning software-assisted transjugular intrahepatic portosystemic shunt: a technical modification. *Cardiovasc Intervent Radiol*. 2015;**38**(3):742–6. doi: 10.1007/s00270-014-0931-0. [PubMed: 24934737].
23. Wallace MJ, Kuo MD, Glaiberman C, Binkert CA, Orth RC, Soulez G, et al. Three-dimensional C-arm cone-beam CT: applications in the interventional suite. *J Vasc Interv Radiol*. 2008;**19**(6):799–813. doi: 10.1016/j.jvir.2008.02.018. [PubMed: 18503893].
24. Luo X, Ye L, Zhou X, Tsauo J, Zhou B, Zhang H, et al. C-Arm Cone-Beam Volume CT in Transjugular Intrahepatic Portosystemic Shunt: Initial Clinical Experience. *Cardiovasc Intervent Radiol*. 2015;**38**(6):1627–31. doi: 10.1007/s00270-015-1087-2. [PubMed: 25832762].
25. Berry K, Lerrigo R, Liou IW, Ioannou GN. Association Between Transjugular Intrahepatic Portosystemic Shunt and Survival in Patients With Cirrhosis. *Clin Gastroenterol Hepatol*. 2016;**14**(1):118–23. doi: 10.1016/j.cgh.2015.06.042. [PubMed: 26192147].
26. Garcia-Pagan JC, Heydtmann M, Raffa S, Plessier A, Murad S, Fabris F, et al. TIPS for Budd-Chiari syndrome: long-term results and prognostics factors in 124 patients. *Gastroenterology*. 2008;**135**(3):808–15. doi: 10.1053/j.gastro.2008.05.051. [PubMed: 18621047].